Thermally activated switching rate of a nanomagnet in the presence of spin torque

Tomohiro Taniguchi,[1] Yasuhiro Utsumi,[2] and Hiroshi Imamura[1]
[1]*National Institute of Advanced Industrial Science and Technology (AIST), Spintronics Research Center, Tsukuba, Ibaraki 305-8568, Japan*
[2]*Faculty of Engineering, Mie University, Tsu, Mie 514-8507, Japan*
(Received 10 July 2013; published 16 December 2013)

The current dependence of the spin torque switching rate in a thermally activated region of an in-plane magnetized system was studied. The logarithm of the switching rate depended nonlinearly on current in the high-current region, $I_c \lesssim I < I_c^*$, where I_c and I_c^* are critical currents distinguishing the stability of the magnetization. We also found that the attempt frequency had a minimum around I_c, and that the attempt frequency at I_c was three orders of magnitude smaller than that at zero current, contrary to the assumption in previous analyses of experiments that it remains constant.

DOI: 10.1103/PhysRevB.88.214414 PACS number(s): 75.78.−n, 05.40.Jc, 75.60.Jk, 85.75.−d

I. INTRODUCTION

The escape problem of a Brownian particle from a metastable state is ubiquitous in many fields of science, such as the chemical reaction of molecules.[1–7] Spin-torque-driven magnetization switching[8,9] in nanostructured ferromagnets in the thermally activated region also belongs to this problem, which has been extensively studied because of its potential application to spintronics devices such as magnetic random access memory (MRAM) and magnetic sensors. The observation of the magnetization switching provides us with important information, such as the retention time of the MRAM. More than a decade has passed since the first experimental and theoretical works on spin torque switching in the thermally activated region.[10–16]

Spin torque switching can be regarded as Brownian motion in the presence of a nonconservative force, contrary to switching by a magnetic field, which is a conservative force defined as the gradient of a potential. The lack of a general method to formulate the switching rate in the presence of the nonconservative force is an unresolved problem in statistical physics.[17,18] Therefore, many assumptions have been made in previous theories of spin torque switching.[14–16] However, recent works[19–24] have revealed the limits of the applicability of previous theories. For example, the switching rate has been assumed to obey the Arrhenius law, $\nu = f e^{-\Delta}$, with linear scaling of the switching barrier, $\Delta = \Delta_0(1 - I/I_c)$, where f, Δ_0, I, and I_c are the attempt frequency, the thermal stability, the current, and the critical current of the precession around the easy axis, respectively.[14–16] However, the linear scaling is valid only in the low-current region,[24] while a relatively large current has been applied in experiments[10–12] to observe the switching quickly. The use of the linear scaling leads to an error of the estimation of the thermal stability.[22] Another issue is that the transition state theory previously adopted[16] cannot estimate the switching rate under a low damping limit,[25] while the Gilbert damping constant of materials typically used in spintronics application is very low,[26] i.e., $\alpha = 10^{-3}$–10^{-2}. These facts prompted us to revisit the theory of spin torque switching in a thermally activated region.

In this paper, we study the spin torque switching rate of an in-plane magnetized system using the mean first passage time approach.[2,3,25,27] The introduction of the effective energy density enables us to calculate the switching rate even in the presence of the nonconservative force. The switching rate showed a nonlinear dependence on the current in the high-current region ($I_c \lesssim I < I_c^*$) on a logarithmic scale, where $I_c^* \simeq 1.27 I_c$ is the spin torque switching current at zero temperature. The attempt frequency was strongly suppressed around I_c contrary to the assumption in previous experimental analysis that it remains constant.[10–12] For example, the attempt frequency at I_c was three orders of magnitude smaller than that at zero current. The theoretical approach presented in this paper is useful for the escape problem of a Brownian particle under a nonconservative force when the magnitude of the nonconservative force is much smaller than that of the conservative force.

The paper is organized as follows. In Sec. II, the Fokker-Planck equation for the magnetization dynamics in the energy space is introduced based on the small damping assumption. In Sec. III, the current dependence of the switching rate, as well as that of the attempt frequency, is calculated by using the mean first passage time approach. Section IV is devoted to the conclusion.

II. FOKKER-PLANCK EQUATION IN ENERGY SPACE

Figure 1(a) schematically shows an in-plane magnetized system, where the x and z axes are normal to the film plane and parallel to the in-plane easy axis, respectively. The unit vectors pointing in the magnetization directions of the free and the pinned layers are denoted as $\mathbf{m} = (\sin\theta\cos\varphi, \sin\theta\sin\varphi, \cos\theta)$ and $\mathbf{n}_p = \mathbf{e}_z$, respectively. Here, we assume that the magnetization dynamics is well described by the macrospin model. The macrospin assumption is, at least for the grand state, guaranteed by the spin torque diode experiment[28] in which the oscillation frequency of the free layer magnetization agrees with the ferromagnetic resonance frequency derived by the macrospin model. The positive current is defined as the electron flow from the free layer to the pinned layer. The energy density of the in-plane magnetized system is

$$E = -\frac{M H_K}{2}(\mathbf{m}\cdot\mathbf{e}_z)^2 + \frac{4\pi M^2}{2}(\mathbf{m}\cdot\mathbf{e}_x)^2, \qquad (1)$$

where M, H_K, and $-4\pi M$ are the magnetization, the uniaxial anisotropy field along the z axis, and the demagnetization field along the x axis, respectively. The magnetic field is defined

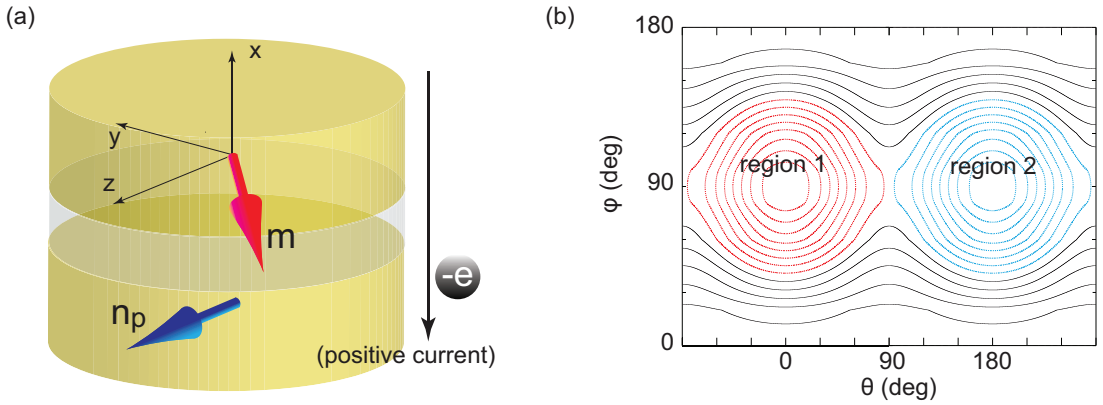

FIG. 1. (Color online) (a) A schematic view of the in-plane magnetized system. The unit vectors pointing in the magnetization directions of the free and the pinned layers are denoted as $\mathbf{m}$ and $\mathbf{n}_{\rm p}$, respectively. The x axis is normal to the film plane and the z axis is parallel to the in-plane easy axis. (b) A schematic view of the constant energy curves. Two low-energy regions are separated by a saddle point. The area outside of regions 1 and 2 (black lines) corresponds to the high-energy region.

as $\mathbf{H} = -\partial E/(\partial M\mathbf{m})$. Figure 1(b) schematically shows the constant energy curves of E in (θ,φ) space. The in-plane magnetized system has two low-energy regions around the energy minima at $\mathbf{m} = \pm\mathbf{e}_z$ corresponding to $E = -MH_{\rm K}/2 \equiv E_{\rm K}$. These two low-energy regions are separated by the saddle point $\mathbf{m} = \pm\mathbf{e}_y$ at which the energy density $E_{\rm s} = 0$. We named the low-energy region, $E_{\rm K} \leqslant E \leqslant E_{\rm s}$, around $\mathbf{m} = +\mathbf{e}_z\,(-\mathbf{e}_z)$ region 1 (2). The area outside regions 1 and 2 corresponds to the high-energy region. The magnetization dynamics is described by the Landau-Lifshitz-Gilbert equation with the random torque,

$$\frac{d\mathbf{m}}{dt} = -\gamma\mathbf{m}\times\mathbf{H} - \gamma H_{\rm s}\mathbf{m}\times(\mathbf{n}_{\rm p}\times\mathbf{m}) - \gamma\mathbf{m}\times\mathbf{h} + \alpha\mathbf{m}\times\frac{d\mathbf{m}}{dt}, \tag{2}$$

where γ and α are the gyromagnetic ratio and the Gilbert damping constant, respectively. The spin torque strength, $H_{\rm s} = \hbar\eta I/(2eMV)$, consists of the current I, the spin polarization η, and the volume of the free layer. The components of the random field, h_k $(k = x,y,z)$, satisfy the fluctuation-dissipation theorem,[29] $\langle h_i(t)h_j(t')\rangle = (2D/\gamma^2)\delta_{ij}\delta(t-t')$, where the diffusion coefficient $D = \alpha\gamma k_{\rm B}T/(MV)$ consists of the Boltzmann constant $k_{\rm B}$ and the temperature T.

During the switching between regions 1 and 2, the magnetization precesses on the constant energy curve around the easy axis. The precession period is determined by the anisotropy fields, $H_{\rm K}$ and $4\pi M$, and is typically on the order of 1 ns.[28] On the other hand, the switching time is determined by the damping, the spin torque, and the random field, and is on the order of 1 μs–1 ms, depending on the current magnitude.[11] Such a long time scale of the switching is due to the fact that the correlation function of the random torque, which induces the switching, is proportional to the small parameter α.[26] Therefore, the precession period on the constant energy curve is much shorter than the switching time. Also, because of the large demagnetization field due to the thin film geometry, as soon as the energy exceeds the saddle points energy, the magnetization moves from region 1 (2) to 2 (1) by the precession around the demagnetization field, and relaxes to region 2 (1). Therefore, the dominant contribution to the switching rate is the time climbing the potential well of region 1 or 2. Thus, we average the magnetization dynamics on the constant energy curve in regions 1 and 2, and we neglect the high-energy region. The averaged dynamics is described by the Fokker-Planck equation in the energy space,[30] which can be derived from Eq. (2) and is given by

$$\frac{\partial\mathcal{P}}{\partial t} + \frac{\partial J}{\partial E} = 0, \tag{3}$$

where $\mathcal{P} = \mathcal{P}(E,t|E',t')$ is the transition probability function of the magnetization direction from the state (E',t') to (E,t). The probability current is

$$J = -\frac{\alpha M\mathscr{M}_\alpha}{\gamma\tau}\frac{d\mathscr{E}}{dE}\mathcal{P} - D\left(\frac{M}{\gamma}\right)^2\mathscr{M}_\alpha\frac{\partial}{\partial E}\frac{\mathcal{P}}{\tau}. \tag{4}$$

We use the approximation $1+\alpha^2 \simeq 1$ because the present theory is based on the small damping assumption. The effective energy density for region i is defined as

$$\mathscr{E}_i(E) = \int_{E_{\rm s}}^{E} dE'\left[1 - \frac{\mathscr{M}_{\rm s}(E')}{\alpha\mathscr{M}_\alpha(E')}\right], \tag{5}$$

where the lower boundary of the integral, $E_{\rm s}$, is chosen to make the effective energy density continuous at the boundary of regions 1 and 2. The precession period on the constant energy curve, $\tau = \oint dt$, and the functions $\mathscr{M}_\alpha = \gamma^2\oint dt[\mathbf{H}^2 - (\mathbf{m}\cdot\mathbf{H})^2]$ and $\mathscr{M}_{\rm s} = \gamma^2 H_{\rm s}\oint dt[\mathbf{n}_{\rm p}\cdot\mathbf{H} - (\mathbf{m}\cdot\mathbf{n}_{\rm p})(\mathbf{m}\cdot\mathbf{H})]$, which are proportional to the energy dissipation due to the damping and the work done by spin torque on the constant energy curve, respectively, are given by

$$\tau = \frac{4}{\gamma\sqrt{H_{\rm K}(4\pi M - 2E/M)}}\mathsf{K}\left(\sqrt{\frac{4\pi M(H_{\rm K}+2E/M)}{H_{\rm K}(4\pi M - 2E/M)}}\right), \tag{6}$$

$$\mathscr{M}_\alpha = 4\gamma\sqrt{\frac{4\pi M - 2E/M}{H_{\rm K}}}\left[\frac{2E}{M}\mathsf{K}\left(\sqrt{\frac{4\pi M(H_{\rm K}+2E/M)}{H_{\rm K}(4\pi M - 2E/M)}}\right) + H_{\rm K}\mathsf{E}\left(\sqrt{\frac{4\pi M(H_{\rm K}+2E/M)}{H_{\rm K}(4\pi M - 2E/M)}}\right)\right], \tag{7}$$

$$\mathscr{M}_s = \pm\frac{2\pi\gamma H_s(H_K + 2E/M)}{\sqrt{H_K(H_K + 4\pi M)}}, \tag{8}$$

where $\mathsf{K}(k)$ and $\mathsf{E}(k)$ are the first and second kind of complete elliptic integrals, respectively. The double sign in Eq. (8) means the upper (+) for region 1 and the lower (−) for region 2. This difference of the sign of $\mathscr{M}_s$ represents the fact that the spin torque for $I > 0$ destabilizes the magnetization in region 1 while it stabilizes the magnetization in region 2.

Equation (4) indicates that, after averaging the magnetization dynamics on the constant energy curve, the switching can be regarded as the Brownian motion on the effective energy density in which the equation of motion with the deterministic force is $(1/\tau)\oint dt(dE/dt) = -[\alpha M\mathscr{M}_\alpha/(\gamma\tau)](d\mathscr{E}_i/dE)$. The thermally activated region is defined by $-d\mathscr{E}/dE < 0$. We note that

$$\lim_{E\to E_K}\frac{d\mathscr{E}_i}{dE} = 1 \mp \frac{I}{I_c}, \tag{9}$$

$$\lim_{E\to E_s}\frac{d\mathscr{E}_i}{dE} = 1 \mp \frac{I}{I_c^*}, \tag{10}$$

respectively, where $I_c = [2\alpha eMV/(\hbar\eta)](H_K + 2\pi M)$ and $I_c^* = [4\alpha eMV/(\pi\hbar\eta)]\sqrt{4\pi M(H_K + 4\pi M)} \simeq 1.27I_c$.[24,31] The physical meanings of I_c and I_c^* are that, for region 1, the state $\mathbf{m} = \mathbf{e}_z$ is destabilized by the current $I > I_c$ while the magnetization switches without the thermal fluctuation for $I > I_c^*$. Therefore, in terms of the current, the thermally activated region is defined by $I < I_c^*$. It should also be noted that the steady-state solution of Eq. (3) in the region i is the Boltzmann distribution with the effective energy density, i.e., $\mathcal{P}/\tau \propto e^{-\mathscr{E}_i(E)V/(k_BT)}$.

Figure 2 shows the typical dependences of $\mathscr{E}_1$ on E for $I \leqslant I_c$ and $I_c < I \leqslant I_c^*$, where the values of the parameters[24] are $M = 1000$ emu/cm^3, $H_K = 200$ Oe, $V = \pi \times 80 \times 35 \times 2.5$ nm^3, $\eta = 0.8$, $\gamma = 1.764 \times 10^7$ rad/(Oe s), and $\alpha = 0.01$, respectively. We denote the energy density corresponding to the local minimum of the effective energy density as E^*, which

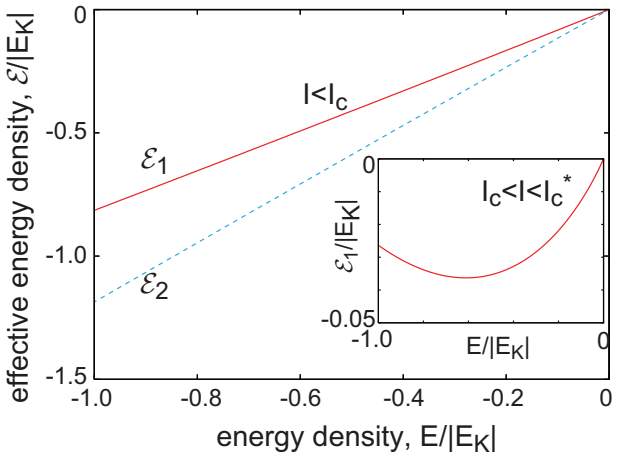

FIG. 2. (Color online) Schematic views of the effective energy density of region 1 ($E_K \leqslant E \leqslant E_s$) in the energy space for $I = 0.2I_c$. Both E and $\mathscr{E}_1$ are normalized by $|E_K| = MH_K/2$. The inset shows $\mathscr{E}_1$ for $I = 0.2(I_c^* - I_c) + I_c$. The dotted line is $\mathscr{E}_2$.

for region 1 is located at

$$E^*(\text{region 1}) = \begin{cases} E_K & (I \leqslant I_c) \\ \text{solution of } d\mathscr{E}_1/dE = 0 & (I_c < I < I_c^*). \end{cases} \tag{11}$$

The minimum of $\mathscr{E}_2$ is always located at $E^* = E_K$.

III. MEAN FIRST PASSAGE TIME APPROACH TO SWITCHING RATE

The mean first passage time,[2,3,27] which characterizes how long the magnetization stays in the energy range $E^* \leqslant E \leqslant E_s$ of the region i, is defined as

$$\mathcal{T}_i(E) = \int_0^\infty dt \int_{E^*}^{E_s} dE_1 \mathcal{P}(E_1, t|E, 0). \tag{12}$$

The equation to determine the mean first passage time is obtained from the adjoint of Eq. (3), and is given by

$$\frac{\alpha M\mathscr{M}_\alpha}{\gamma\tau}\frac{d\mathscr{E}_i}{dE}\frac{d\mathcal{T}_i}{dE} - D\left(\frac{M}{\gamma}\right)^2\frac{1}{\tau}\frac{d}{dE}\mathscr{M}_\alpha\frac{d\mathcal{T}_i}{dE} = 1. \tag{13}$$

We use the reflecting and the absorbing boundary conditions[2,3,27] at $E = E^*$ and $E = E_s$, respectively: that is, $d\mathcal{T}_i(E^*)/dE = 0$ and $\mathcal{T}_i(E_s) = 0$. Then, the mean first passage time is given by

$$\mathcal{T}_i(E) = \frac{\gamma V}{\alpha M k_B T}\int_E^{E_s} dE_1 \int_{E^*}^{E_1} dE_2 \frac{\tau(E_2)}{\mathscr{M}_\alpha(E_1)} \times \exp\left\{\frac{[\mathscr{E}_i(E_1) - \mathscr{E}_i(E_2)]V}{k_BT}\right\}. \tag{14}$$

The switching rate from region i to region j is

$$\nu_{ij} = \frac{d\mathscr{E}_j(E_s)/dE}{d\mathscr{E}_i(E_s)/dE + d\mathscr{E}_j(E_s)/dE}\frac{1}{\mathcal{T}_i(E^*)}. \tag{15}$$

Here, we assume that once the magnetization reaches the saddle point, the probability of it moving to regions i or j is proportional to the gradient of the effective energy, i.e., the deterministic force acting on a Brownian particle.[32] For a conservative system,[2] Eq. (15) is $1/(2\mathcal{T}_i)$. The switching probability P and the switching current distribution dP/dI measured in the experiments can be calculated from Eq. (15). For example, for $I > 0$, the switching probability from $\mathbf{m} = \mathbf{e}_z$ to $\mathbf{m} = -\mathbf{e}_z$ is $P \simeq 1 - e^{-\int_0^t \nu_{12}(t')dt'}$. It should be noted that $\lim_{I\to I_c^*}\mathcal{T}_1(E^*) = 0$ because region 1 is no longer stable due to the spin torque; thus, the magnetization immediately switches to region 2. For the same reason, $\lim_{I\to I_c^*}\nu_{21} = 0$.

Equations (14) and (15) indicate that the switching rate cannot be expressed as the Arrhenius law, in general. However, it is convenient to introduce the switching barrier and the attempt frequency as

$$\Delta_i = \frac{[\mathscr{E}_i(E_s) - \mathscr{E}_i(E^*)]V}{k_BT}, \tag{16}$$

$$f_{ij} = \nu_{ij}e^{\Delta_i}. \tag{17}$$

The current dependence of the switching barrier was extensively studied in Ref. 24. In the low-current region,

$I < I_c$, corresponding to the high barrier limit, $\Delta_i \gg 1$,[33] the exponential terms in Eq. (14) are dominated by $E_1 = E_s$ and $E_2 = E_K$, respectively. Using the Taylor expansion of $\mathscr{E}_i$, $\mathcal{T}_i$ can be approximated as

$$\mathcal{T}_i(E_K) \simeq \frac{\gamma k_B T \tau(E_K) e^{\Delta_i}}{\alpha M V \mathscr{M}_\alpha(E_s)[d\mathscr{E}_i(E_K)/dE][d\mathscr{E}_i(E_s)/dE]}, \tag{18}$$

where $\mathscr{M}_\alpha(E_s) = 4\gamma\sqrt{H_K 4\pi M}$ and $\tau(E_K) = 2\pi/[\gamma\sqrt{H_K(H_K + 4\pi M)}]$. Then, the switching rate obeys the Arrhenius law as follows:

$$\nu_{ij} = \frac{\alpha M V \mathscr{M}_\alpha(E_s)}{2\gamma k_B T \tau(E_K)}\left(1 \mp \frac{I}{I_c}\right)\left[1 - \left(\frac{I}{I_c^*}\right)^2\right] \times \exp\left[-\Delta_0\left(1 \mp \frac{I}{\tilde{I}_c}\right)\right], \tag{19}$$

where $\Delta_0 = M H_K V/(2k_B T)$ is the thermal stability. The term $(1 \mp I/I_c)$ of Eq. (19) arises from $d\mathscr{E}_1(E_K)/dE$ in Eq. (18) while the term $[1 - (I/I_c^*)^2]$ of Eq. (19) arises from $d\mathscr{E}_i(E_s)/dE$ in Eqs. (15) and (18), respectively. The current $\tilde{I}_c$ is defined as $I/\tilde{I}_c = \int_{E_K}^{E_s}(dE/|E_K|)\mathscr{M}_s/(\alpha\mathscr{M}_\alpha)$, which satisfies $I_c < \tilde{I}_c < I_c^*$. Although the linear scaling of the switching barrier appears in this low-current region, the scaling current is not the switching current, as argued in Refs. 14–16. This means that the previous analyses of the experiments underestimate the real value of the switching current.[10,11,14,15,34] Equation (19) can be directly reproduced by applying Brown's approach[29] to Eq. (3), as shown in the Appendix.

Equation (19) becomes zero in the zero-dissipation limit ($\alpha \to 0$) because the correlation function of the thermal field, which induces the switching, is proportional to α according to the fluctuation-dissipation theorem. However, the switching rate based on the transition state theory[16] given by $\nu_{ij} = \exp[-\Delta_0(1 \mp I/I_c)]/\tau(E_K)$ remains finite in the zero-dissipation limit. This problem has already been pointed out in the case of the magnetic field switching.[25] The terms except for $1/\tau(E_K)$ in Eq. (19) can be regarded as correction terms to the transition state theory used in Ref. 16.

Figure 3(a) shows the dependence of the switching rate ν_{ij} on the current numerically obtained from Eq. (14), where ν_{ij} are normalized by the values at $I = 0$. The values of the parameters are those used in Fig. 2 with $T = 300$ K. The analytical solution, Eq. (19), for $I < I_c$ is shown by dots, and it shows good agreement with the numerical result. The switching rate in the high-current region, $I_c < I < I_c^*$, is shown in Fig. 3(b). One of the main results in this paper is the nonlinear dependence of ν_{ij} in the relatively high-current region on the logarithmic scale, while the linear dependence has been widely used in previous works[14,15] by assuming the linear scaling of the switching barrier and the constant attempt frequency.

The current dependence of the attempt frequency, f_{ij}, is shown in Fig. 4. The attempt frequency, f_{12}, decreases with increasing current for $I \lesssim I_c$, while it increases for $I_c \lesssim I < I_c^*$. The discontinuity of the slope of f_{12} around I_c arises for the following reason. According to Eqs. (15) and (18), the

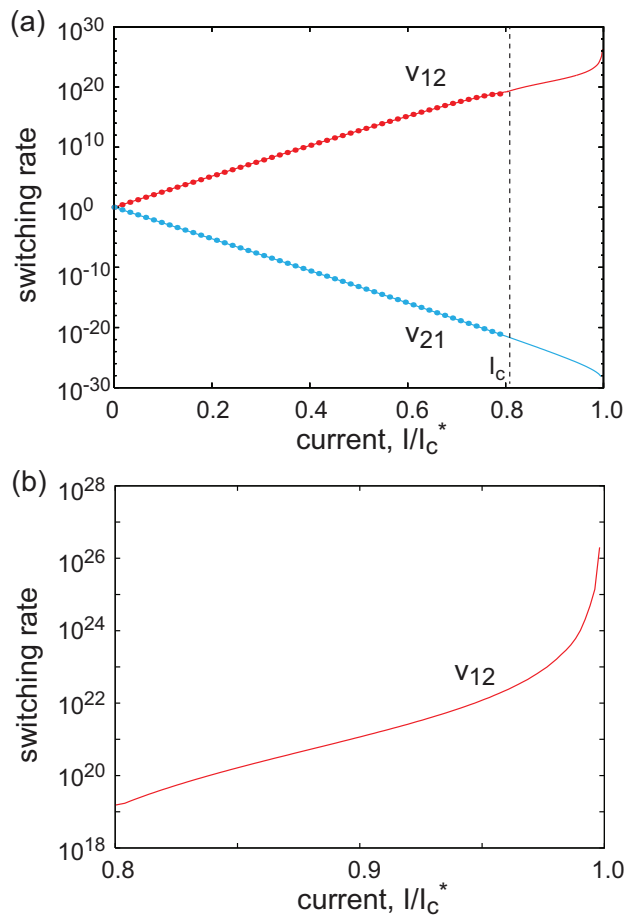

FIG. 3. (Color online) (a) Dependence of the switching rate ν_{ij} on the current I. The values are normalized by those at $I = 0$, while the current is normalized by I_c^*. The dots represent the analytical solutions derived in the region $I < I_c$. The dashed line represents the position of I_c ($I_c/I_c^* \simeq 0.81$). (b) An enlarged view of the switching rate in the high-current region, $I_c < I < I_c^*$.

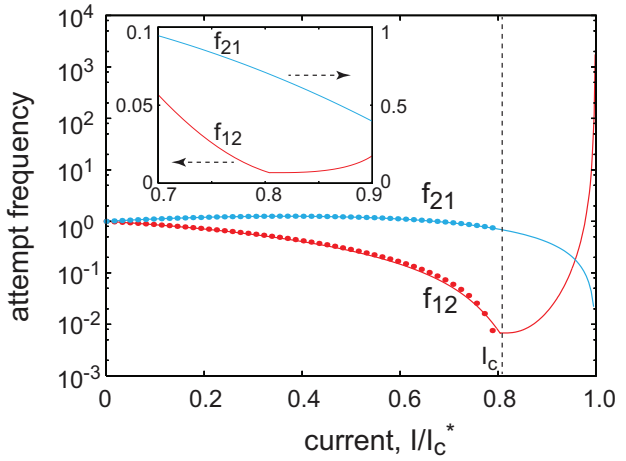

FIG. 4. (Color online) Dependence of the attempt frequency, f_{ij}, on the current. The values are normalized by those at $I = 0$, while the current is normalized by I_c^*. The dots represent the analytical solutions obtained from Eq. (19). The dashed line represents the position of I_c ($I_c/I_c^* \simeq 0.81$). The inset shows the linear plots of f_{12} and f_{21} around I_c.

attempt frequency for $I < I_c$ is approximately proportional to the gradient of $\mathscr{E}_1$ at its minimum, $d\mathscr{E}_1(E_K)/dE$, which decreases with increasing current. Here, $d\mathscr{E}_1(E_K)/dE$ arises from the Taylor expansion of $\mathscr{E}_1$ in Eq. (14). On the other hand, $d\mathscr{E}_1/dE$ for $I_c \lesssim I < I_c^*$ is zero at the minimum of $\mathscr{E}_1$ as shown by Eq. (11). Then, f_{12} is approximately proportional to the curvature of $\mathscr{E}_1$ at its minimum, $d^2\mathscr{E}_1(E^*)/dE^2$, which increases with increasing the current. Thus, the attempt frequency shows a minimum around I_c. The attempt frequency in Fig. 4 depends strongly on the current. For example, the attempt frequency at I_c is three orders of magnitude smaller than that at zero current. Contrary to this result, the attempt frequency has been generally assumed to be constant in previous experimental analyses.[10–15]

IV. CONCLUSION

In summary, the spin torque switching rate of an in-plane magnetized system was studied. The current dependence of the switching rate was obtained numerically, and an analytical formula in the low-current region was derived. The logarithm of the switching rate depends nonlinearly on the current in the high-current region. The switching barrier depends linearly on the current in the low-current region, which guarantees the validity of the previous theories,[14–16] although the scaling current $\tilde{I}_c$ is not identical to the switching current. The attempt frequency has a minimum around the critical current I_c, and exhibits a strong current dependence while it has been assumed to be constant in previous experimental analyses.

ACKNOWLEDGMENTS

The authors would like to acknowledge M. Marthaler, D. S. Golubev, H. Sukegawa, T. Yorozu, H. Kubota, H. Maehara, A. Emura, T. Nozaki, M. Konoto, K. Yakushiji, A. Fukushima, K. Ando, and S. Yuasa for the valuable discussions they had with us. This work was supported by JSPS KAKENHI Grant-in-Aid for Young Scientists (B) 25790044.

APPENDIX: BROWN'S APPROACH TO EQ. (19)

The switching rate in the high barrier limit, Eq. (19), can be obtained by using Brown's approach.[29] Toward that end, it is convenient to use $W = M\mathcal{P}/(\gamma\tau)$ instead of $\mathcal{P}$. In terms of W, Eqs. (3) and (4) can be expressed as

$$\frac{\gamma\tau}{M}\frac{\partial W}{\partial t} + \frac{\partial J}{\partial E} = 0, \tag{A1}$$

$$J = -\frac{\alpha k_B T}{V}\mathscr{M}_\alpha e^{-\mathscr{E}V/(k_B T)}\frac{\partial}{\partial E}e^{\mathscr{E}V/(k_B T)}W. \tag{A2}$$

To guarantee $\Delta_i \gg 1$, we assume that $I < I_c$, i.e., $E^* = E_K$. Then, Δ_i is given by $\Delta = \Delta_0(1 \mp I/\tilde{I}_c)$. In the high barrier limit, the probability functions near the minima of $\mathscr{E}$ are approximately the Boltzmann distribution functions, while a tiny constant flow of the probability current crosses over the saddle point. The probability functions of regions 1 and 2 around E_K are expressed as

$$W_i(E) = W_i(E_K)\exp\left\{-\frac{[\mathscr{E}_i(E) - \mathscr{E}_i(E_K)]V}{k_B T}\right\}, \tag{A3}$$

where $i = 1,2$, $W_i(E_K) = W_i(E_s)\exp\{[\mathscr{E}_i(E_s) - \mathscr{E}_i(E_K)]V/(k_B T)\}$, and $W_i(E_s)$ is the probability function at the saddle point satisfying $W_1(E_s) = W_2(E_s)$. Since the probability functions show sharp peaks around E_K, and rapidly decrease by approaching E_s, the integrals of the probability functions,

$$n_i = \frac{\gamma}{M}\int_{E_K}^{E_i} dE\, W_i(E)\tau(E), \tag{A4}$$

are independent of the upper boundaries, E_i, which are arbitrary points located in regions 1 and 2 close to E_s. Equation (A4) can be expressed as $n_i = W_i(E_K)\exp[\mathscr{E}_i(E_K)V/(k_B T)]I_i$, where I_i are given by

$$I_i = \frac{\gamma}{M}\int_{E_K}^{E_1} dE \exp\left[-\frac{\mathscr{E}_i(E)V}{k_B T}\right]\tau(E). \tag{A5}$$

The exponential term in Eq. (A5) rapidly decreases from $E = E_K$ to $E = E_s$. Thus, by using the Taylor expansion of $\mathscr{E}_i$ around $E = E_K$ and using the fact that $\lambda_E^* = -d\mathscr{E}_i/dE \neq 0$ for $I < I_c$, I_i can be approximated to

$$I_i \simeq \frac{\gamma k_B T\tau(E_K)}{MV[d\mathscr{E}_i(E_K)/dE]}e^{-\mathscr{E}_i(E_K)V/(k_B T)}. \tag{A6}$$

The double sign means the upper for region 1 and the lower for region 2.

Next, we consider the flow of the probability current from region 1 to region 2 crossing the saddle point. Equation (A2) can be rewritten as

$$\frac{JV}{\alpha k_B T\mathscr{M}_\alpha}e^{\mathscr{E}(E)V/(k_B T)} = -\frac{\partial}{\partial E}e^{\mathscr{E}(E)V/(k_B T)}W. \tag{A7}$$

By assuming the divergenceless current,[29] the integral of Eq. (A7) over $[E_1, E_s]$ is given by

$$\frac{JV}{\alpha k_B T}\int_{E_1}^{E_s} dE\frac{e^{\mathscr{E}_1(E)V/(k_B T)}}{\mathscr{M}_\alpha} = W_1(E_1)e^{\mathscr{E}_1(E_1)V/(k_B T)} - W_1(E_s)e^{\mathscr{E}_1(E_s)V/(k_B T)}. \tag{A8}$$

We also integrate Eq. (A7) over $[E_2, E_s]$ by changing the sign of the probability current J. Then, we obtain the following equation;

$$\frac{JV}{\alpha k_B T}I_\alpha = W_1(E_1)e^{\mathscr{E}_1(E_1)V/(k_B T)} - W_2(E_2)e^{\mathscr{E}_2(E_2)V/(k_B T)}, \tag{A9}$$

where the right-hand side is identical to $(n_1/I_1) - (n_2/I_2)$. On the other hand, I_α is given by

$$I_\alpha = \int_{E_1}^{E_s} dE\frac{e^{\mathscr{E}_1(E)V/(k_B T)}}{\mathscr{M}_\alpha} + \int_{E_2}^{E_s} dE\frac{e^{\mathscr{E}_2(E)V/(k_B T)}}{\mathscr{M}_\alpha} \simeq \frac{k_B T}{\mathscr{M}_\alpha(E_s)V}\left[\frac{e^{\mathscr{E}_1(E_s)V/(k_B T)}}{d\mathscr{E}_1(E_s)/dE} + \frac{e^{\mathscr{E}_2(E_s)V/(k_B T)}}{d\mathscr{E}_2(E_s)/dE}\right]. \tag{A10}$$

The probability current satisfies $dn_1/dt = -dn_2/dt = -J$. Thus, we obtain the following rate equation between regions 1 and 2:

$$\frac{dn_1}{dt} = -\frac{dn_2}{dt} = -n_1\nu_{12} + n_2\nu_{21}, \tag{A11}$$

where the switching rate from region i to region j is $\nu_{ij} = \alpha k_B T/(I_i I_\alpha V)$. By using Eqs. (9), (10), (A6), and (A10), the explicit form of the switching rate is given by

$$\nu_{ij} = \frac{\alpha M V \mathscr{M}_\alpha(E_s)}{2\gamma k_B T \tau(E_K)}\left(1 \mp \frac{I}{I_c}\right)\left[1 - \left(\frac{I}{I_c^*}\right)^2\right] e^{-\Delta_i}, \quad \text{(A12)}$$

where the double sign means the upper for $(i,j) = (1,2)$ and the lower for $(2,1)$. Equation (A12) is identical to Eq. (19). The solutions of Eq. (A11) for constant current in time with the initial condition $n_1(t=0) = 1$ and $n_2(t=0) = 0$ are given by

$$n_1 = \frac{\nu_{21}}{\nu_{12}+\nu_{21}} + \frac{\nu_{12}}{\nu_{12}+\nu_{21}} e^{-(\nu_{12}+\nu_{21})t}, \quad \text{(A13)}$$

$$n_2 = \frac{\nu_{12}}{\nu_{12}+\nu_{21}} - \frac{\nu_{12}}{\nu_{12}+\nu_{21}} e^{-(\nu_{12}+\nu_{21})t}. \quad \text{(A14)}$$

For the positive current, $\nu_{12} \gg \nu_{21}$, and therefore $n_1 \simeq e^{-\nu_{12}t}$ and $n_2 = 1 - e^{-\nu_{12}t}$, where n_2 corresponds to the switching probability measured in the experiments.

[1] P. Hänggi, J. Stat. Phys. **42**, 105 (1986).
[2] P. Hänggi, P. Talkner, and M. Borkovec, Rev. Mod. Phys. **62**, 251 (1990).
[3] C. W. Gardiner, *Stochastic Methods: A Handbook for the Natural and Social Sciences*, 4th ed. (Springer, Berlin, 2009).
[4] G. I. Bell, Science **200**, 618 (1978).
[5] H. Dekker, Physica A **135**, 80 (1986).
[6] G. Hummer and A. Szabo, Biophys. J. **85**, 5 (2003).
[7] J. Husson and F. Pincet, Phys. Rev. E **77**, 026108 (2008).
[8] J. C. Slonczewski, J. Magn. Magn. Mater. **159**, L1 (1996).
[9] L. Berger, Phys. Rev. B **54**, 9353 (1996).
[10] F. J. Albert, N. C. Emley, E. B. Myers, D. C. Ralph, and R. A. Buhrman, Phys. Rev. Lett. **89**, 226802 (2002).
[11] S. Yakata, H. Kubota, T. Sugano, T. Seki, K. Yakushiji, A. Fukushima, S. Yuasa, and K. Ando, Appl. Phys. Lett. **95**, 242504 (2009).
[12] D. Bedau, H. Liu, J. Z. Sun, J. A. Katine, E. E. Fullerton, S. Mangin, and A. D. Kent, Appl. Phys. Lett. **97**, 262502 (2010).
[13] X. Cheng, C. T. Boone, J. Zhu, and I. N. Krivorotov, Phys. Rev. Lett. **105**, 047202 (2010).
[14] R. H. Koch, J. A. Katine, and J. Z. Sun, Phys. Rev. Lett. **92**, 088302 (2004).
[15] Z. Li and S. Zhang, Phys. Rev. B **69**, 134416 (2004).
[16] D. M. Apalkov and P. B. Visscher, Phys. Rev. B **72**, 180405 (2005).
[17] D. L. Stein, R. G. Palmer, J. L. van Hemmen, and C. R. Doering, Phys. Lett. A **136**, 353 (1989).
[18] R. S. Maier and D. L. Stein, Phys. Rev. Lett. **69**, 3691 (1992).
[19] *Nanomagnetism and Spintronics*, edited by T. Shinjo (Elsevier, Amsterdam, 2009), Chap. 3.
[20] D. Pinna, A. Mitra, D. L. Stein, and A. D. Kent, Appl. Phys. Lett. **101**, 262401 (2012).
[21] D. Pinna, A. D. Kent, and D. L. Stein, Phys. Rev. B **88**, 104405 (2013).
[22] T. Taniguchi and H. Imamura, Phys. Rev. B **83**, 054432 (2011).
[23] T. Taniguchi, M. Shibata, M. Marthaler, Y. Utsumi, and H. Imamura, Appl. Phys. Express **5**, 063009 (2012).
[24] T. Taniguchi, Y. Utsumi, M. Marthaler, D. S. Golubev, and H. Imamura, Phys. Rev. B **87**, 054406 (2013).
[25] W. T. Coffey and Y. P. Kalmykov, J. Appl. Phys. **112**, 121301 (2012).
[26] M. Oogane, T. Wakitani, S. Yakata, R. Yilgin, Y. Ando, A. Sakuma, and T. Miyazaki, Jpn. J. Appl. Phys. **45**, 3889 (2006).
[27] T. Taniguchi and H. Imamura, Phys. Rev. B **85**, 184403 (2012).
[28] A. A. Tulapurkar, Y. Suzuki, A. Fukushima, H. Kubota, H. Maehara, K. Tsunekawa, D. D. Djayaprawira, N. Watanabe, and S. Yuasa, Nature (London) **438**, 339 (2005).
[29] W. F. Brown, Jr., Phys. Rev. **130**, 1677 (1963).
[30] *Fluctuating Nonlinear Oscillators*, edited by M. Dykman (Oxford University Press, Oxford, 2012), Chap. 6.
[31] *Spin Dynamics in Confined Magnetic Structures III*, edited by B. Hillebrands and A. Thiaville (Springer, Berlin, 2006), p. 272.
[32] By using the boundary condition $\partial(\mathcal{P}/\tau)/\partial E = 0$ and the continuity of J at $E = E_s$, the probability in the region i close to the saddle point is given by $(d\mathscr{E}_j/dE)/[(d\mathscr{E}_i/dE) + (d\mathscr{E}_j/dE)]$, which determines the rate moving to the region j.
[33] For MRAM application, a thermal stability Δ_0 larger than 40 is required. In such a sample, the switching barrier at $I = I_c$ is on the order of unity.
[34] T. Taniguchi and H. Imamura, Appl. Phys. Express **6**, 103005 (2013).